M&C 2017 - International Conference on Mathematics & Computational Methods Applied to Nuclear Science & Engineering, Jeju, Korea, April 16-20, 2017, on USB (2017)

A Nonintrusive POD Approach for High Dimensional Problems using Sparse Grids

F. Alsayyari, D. Lathouwers, J.L. Kloosterman

Department of Nuclear Energy and Radiation Applications, Delft University of Technology, Mekelweg 15, 2629 JB Delft, The Netherlands
f.s.s.alsayyari@tudelft.nl

Abstract - *Reduced order models are effective in reducing the computational burden of large-scale complex systems. Proper Orthogonal Decomposition (POD) is one of the most important methods for such application. Nevertheless, problems parametrized on high dimensional spaces require computations of an enormous number of simulations in the offline phase. In this paper, the use of sparse grids is suggested to select the sampling points in an efficient manner. The method exploits the hierarchical nature of the Smolyak algorithm to select the sparse grid level based on the singular values of the POD basis. Then, a nonintrusive reduced order model is built using Smolyak's combination technique. The proposed method was tested and compared with Radial Basis Functions in two nuclear applications. The first was a one-dimensional slab solved as a diffusion eigenvalue problem and the second was the two-dimensional IAEA benchmark problem. In both cases, the results showed that while Radial Basis Functions resulted in a faster reduced order model, Smolyak's model provided superior accuracy.*

I. INTRODUCTION

Modeling nuclear reactors is a challenging task that involves capturing the interaction between multi-physics phenomena occurring at various scales. In the reactor design process, high fidelity simulation tools are often used to provide a comprehensive solution for the coupled inter-disciplinary problem. Nevertheless, even with the increasing power of today's supercomputers, high fidelity models require a tremendous amount of computational time and memory allocation. For applications of design optimization, uncertainty quantification and control, where many repeated model evaluations are needed, such models are rendered extremely expensive.

Reduced Order Modeling is an effective technique to reduce the dimensionality of large-scale complex systems. The reduction is achieved by replacing the high fidelity model with a low-dimensional efficient model capturing the prominent dynamics of the system. The reduced model can then be used to provide fast solutions with a controlled level of accuracy. Different reduced order modeling techniques can be found in the literature. However, Proper Orthogonal Decomposition (POD) is the favoured method for nonlinear systems [1]. POD was first introduced as a statistical technique to extract dominant characteristics from a set of data. The idea was to represent the data with a set of basic principle components. As a reduced order method, the method was later developed by Lumely [2] to model coherent structures in turbulent flow. The POD method is based on sampling the high fidelity model at several points in the parameter space to construct the so-called snapshot matrix. Then, a reduced basis is created through a Singular Value Decomposition (SVD). The original high fidelity model is then projected onto the created reduced basis space by means of a Galerkin projection. The generation of the snapshot matrix and the building of the model are accomplished in the offline phase, which is executed only once. Afterwards, in the online phase, the generated reduced model can be run inexpensively at any desired parameter point. In reactor physics applications, POD model order reduction was applied to the eigenvalue problem of the diffusion equation in Ref. [3] and to the time-dependent diffusion equation in Ref. [4].

However, projection-based POD methods are code intrusive, which is a major limitation. For legacy codes where access to the governing equations is not possible, the approach is not applicable. For such cases, a slightly different nonintrusive POD technique can be employed. The idea is to benefit from the orthogonality of the subspace basis to generate the Galerkin expansion coefficients at the sampled points. Thus, the coefficient values at the snapshots points are computed without any projection. Then, a surrogate model can be constructed to compute the solution at any required non-sampled point. In literature, different surrogate models have been suggested to compute the expansion coefficients. For lower dimensional problems, direct interpolation or splines can be used as in Ref. [5]. On the other hand, high-dimensionality problems require more advanced techniques. Radial Basis Function (RBF) is one of the commonly used methods in such applications [6].

Nevertheless, the accuracy of the POD method to provide a solution at a non-sampled point is directly affected by the choice of the sampling scheme. The snapshots need to capture the entire dynamics of the model within the desired range. Moreover, in the nonintrusive approach, the sampling points should be dense enough for the surrogate model to reproduce a reliable predictive solution at non-sampled locations. Thus, for nonintrusive methods, the sampling strategy becomes even more relevant. In addition, problems parametrized on high dimensional spaces are prone to the curse of dimensionality, i.e. the exponential increase of the computational time with the increase in the number of dimensions. In these cases, the efficient selection of the sampling points is crucial for any practical application. Latin Hypercube Sampling (LHS) can be an efficient sampling technique to address this issue. However, the lack of adaptivity can be limiting in nonlinear cases. An extension of LHS was suggested in Ref. [7]. The technique improves the initial snapshot matrix by adaptively

selecting new points based on the "influence" of the new point on the snapshot matrix.

In this paper, a different sampling method based on sparse grids is suggested. Sparse grids were first introduced by Smolyak [8] and, ever since, has been used to cope with the curse of dimensionality in multivariate integrations and interpolations. It involves preserving the interpolation property for the unidimensional formula by a specific combination of the tensorized product [9]. In the context of reduced order models, sparse grids were suggested by Peherstorfer [10] to be used as a machine learning tool to build a reduced order model. The approach was tested on heat transfer problems. Also, Xiao [11] presented a method of propagating the expansion coefficients through time with the use of a sparse grid interpolant. The method was tested on the Navier-Stokes equations. This paper, however, presents an approach to exploit the hierarchical nature of the Smolyak's algorithm and select the sparse grid level based on the singular values of the POD basis. Then, an efficient surrogate reduced order model is built using a Smolyak interpolant. The approach can be extended to higher dimensional problems inexpensively. Although the nonintrusive approach is considered in this paper, it is important to note that the proposed sampling method can equally be combined with a Galerkin-POD approach. In this work, the method is tested on two cases. The first is a one-dimensional diffusion eigenvalue problem and the second is the 2D IAEA benchmark problem. A comparison between Smolyak's interpolant and RBF method is presented.

II. THEORY

1. Proper Orthogonal Decomposition

In nonintrusive applications, the high fidelity model is considered as a black box mapping a given input to the desired output. The model, thus, can be seen as an unknown objective function $f : [0\ 1]^d \rightarrow \mathbb{R}$, where d is the dimension of the input defined in the unit hypercube. The objective function $f(x; \lambda)$ is dependent on state x and the input parameters of interest λ. In a Galerkin expansion, the function can be written as a linear combination of basis functions:

$$f(x; \lambda) = \sum_{i=1}^{r} c_i(\lambda)\ u_i(x) \tag{1}$$

where c_i are the expansion coefficients which depend on the input parameter λ and $u_i(x)$ are the basis functions.

The POD method seeks an approximation of the objective function that minimizes the error in L_2 norm [12],

$$\min\ e = \left\| f(x) - \sum_{i=1}^{k} c_i\ u_i(x) \right\|_{L2} \tag{2}$$

The basis functions are chosen such that they are orthonormal. Thus, the coefficients c_i can be computed as follows:

$$c_i = \int_{\Omega} f(x)\ u_i(x) d\Omega \tag{3}$$

Assuming that the objective function is discretized in space, the solution to the minimization problem can be reached with the Singular Value Decomposition (SVD) as follows [6]:

1. sample the objective function at some preselected sampling points λ_k;

2. arrange the solutions to construct the snapshot matrix $M = \{f(\lambda_1), f(\lambda_2), ..., f(\lambda_p)\}$, where p is the number of simulations;

3. perform Singular Value Decomposition on the snapshot matrix $M \rightarrow UDV$ to obtain a matrix U whose columns are the left singular vectors, matrix V whose columns are right singular vectors and a diagonal matrix D with entries σ_k corresponding to the singular values of the snapshot matrix arranged in a descending order.

If the number of non-zero singular values is w, it can be shown that the rank of the snapshot matrix is also w. The POD basis vectors (modes) can be selected as the first r left singular vectors of the matrix U (where $r \leq w$). If r is chosen to be strictly less than w, an approximation error can be quantified using the singular values (σ),

$$E = \frac{\sum_{k=r+1}^{j} \sigma_k^2}{\sum_{k=1}^{j} \sigma_k^2} \tag{4}$$

2. Sparse Grids

The snapshots for the POD method can be generated by different methods depending on the sampling scheme. However, computing the objective function at every possible combination is unrealistic, especially for high dimensional problems. Therefore, in this paper, the sampling points are generated on a sparse grid. The idea is to select a set of nodes for each dimension in the parameter space. Then, the points are tensorized in a specific way to construct the sparse grid. Many choices are possible for the unidimensional nodes. The only requirement is to choose the nodes in a nested manner, i.e. $X_i \subset X_{i+1}$ where X_i is the set of nodes for a given index i. An overview of different possible sparse grid choices can be found in [13].

In this work, the sparse grid is combined with the POD method in order to build a nonintrusive model. This imposes an additional constraint on the selection of the unidimensional nodes. This is because the nodes need to be separated enough in the parameter space to produce enriched POD modes covering the complete range of dynamics of the system. Nevertheless, such selection of nodes might not be the ideal scheme for the interpolation. In many studies, Chebyshev nodes were found to perform better than uniform sampling [13]. However, Chebyshev nodes produce more points very close to each other at the boundary and fewer points in the central region. This increases the risk of overlooking some of the dynamics at the inner region. Therefore, in order to achieve maximum separation of points over the entire parameter domain, equidistant nodes are chosen to generate the sampling points with the

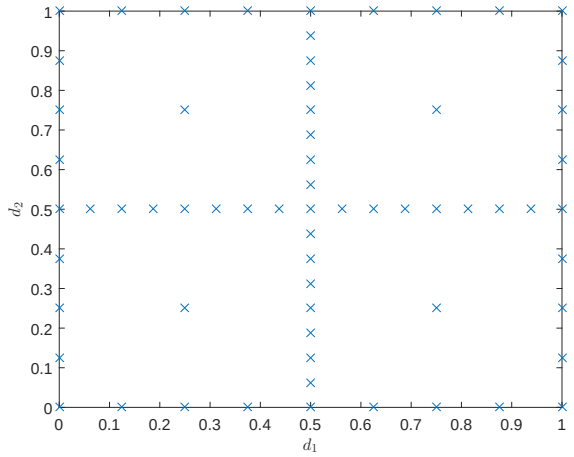

Fig. 1. Sparse grid points for $d = 2$ and $l = 4$.

following formula:

$$m_i = \begin{cases} 1 & \text{if } i = 0 \\ 2^{i-1} + 1 & \text{if } i > 0 \end{cases}$$
$$x_j^i = \begin{cases} \dfrac{j-1}{m_i - 1} & \text{for } j = 1, 2, ..., m_i \quad \text{if } m_i > 1 \\ 0.5 & \text{for } j = 1 \qquad\qquad\quad \text{if } m_i = 1 \end{cases} \tag{5}$$

Where i is the index for any dimension d and x_j^i are the nodes in set X_i. The points are generated in the hypercube $[0\ 1]^d$ which can then be scaled accordingly.

The Smolyak algorithm can be applied to combine the unidimensional nodes into a sparse grid by satisfying the following condition:

$$q - d + 1 \leq |i| \leq q \tag{6}$$

Where d is the dimension, and $|i| = i_1 + i_2 + ... + i_d$ with i_d being an integer index in dimension d. q is a parameter such that $q \geq d$. The level (l) of the sparse grid can be defined by $l = q - d$. Figure 1 shows the sparse grid for $d = 2$ and $l = 4$. Table I presents the number of points for the first 7 levels for different dimensions.

The generated points can then be used to construct the snapshot matrix for the POD. One can select the level to have the maximum affordable number of snapshots. However, we propose an adaptive level selection by computing the SVD for each level successively and setting a criterion based on the decay of the singular values. The concept is based on the fact that the singular values are representative of the energy of each POD mode [12]. Thus, higher singular values indicate POD modes that are contributing more and are considered more important than modes with lower values. Consequently, adding points to the snapshot which result only in lower singular values is analogous to including higher order terms in a Taylor expansion.

TABLE I. Number of sparse grid points by level and dimension.

Level (l)	$d = 2$	$d = 3$	$d = 4$	$d = 5$	$d = 6$
0	1	1	1	1	1
1	5	7	9	11	13
2	13	25	41	61	85
3	29	69	137	241	389
4	65	177	401	801	1457
5	145	441	1105	2433	4865
6	321	1073	2929	6993	15121

Therefore, after a sufficient number of points, the main dynamics is captured and any added point will only change the lower singular values. Thus, benefiting from the hierarchical nature of the sparse grids, we suggest comparing the slope of decay for the leading singular values with each level increase. Then, the appropriate level is selected when no change in the slopes is observed. However, the "leading" singular values still need to be defined properly. In the proposed algorithm, they are defined with respect to the highest singular value, i.e. the first singular values within a margin of the highest singular value (σ_i/σ_1). The margin in this work was taken as 10^{-4}.

Thus, the following algorithm is proposed to select the minimum sparse grid level needed to build a reduced model:

Algorithm
Starting with $l = 1$

1. generate the sparse points for level l;
2. sample the model at the generated points;
3. construct the snapshot matrix;
4. perform the SVD on the snapshots;
5. compute the logarithmic decay slope for the leading singular values;
6. compare the computed decay slope with that of level $l-1$. If the absolute difference is more than a given tolerance, increase l and repeat step 1; otherwise, return U and D .

The algorithm returns the POD modes in the left singular matrix U and the singular values in the diagonal of D. Equation 4 can be used to choose the number of POD modes (r) appropriately. The expansion coefficients (c_i) can be computed from Equation 3 for all parameter points within the training set. Then, in order to compute the solution for a new parameter value, one needs to interpolate between the obtained coefficients. However, interpolation for high dimensional functions is challenging. Therefore, Smolyak's combination technique is used to tensorize unidimensional interpolation functions. Due to the selection of equally spaced nodes, local piecewise multilinear functions are chosen as basis functions. The piecewise linear functions are defined as follows [13]:

$$a_{x_1} = 1 \quad \text{if } i = 1$$
$$a_{x_i^j}(x) = \begin{cases} 1 - (m_i - 1) \cdot |x - x_j^i| & \text{if } |x - x_j^i| < \dfrac{1}{m_i - 1} \\ 0 & \text{otherwise} \end{cases} \tag{7}$$

Where $a(x)$ is the local basis function and m_i is defined as in Eq. 5. The interpolant for one dimension can then be computed as follows:

$$U^i(f) = \sum_{x_i \in X_i} a_{x^i}(x) f(x) \tag{8}$$

Then, as shown in [9], the Smolyak combination technique can be used to construct the multidimensional interpolant:

$$A_{q,d} = \sum_{q-d+1 \le |i| \le q} (-1)^{q-|i|} \binom{d-1}{q-|i|} (U^{i_1}(f) \otimes ... \otimes U^{i_d}(f)) \tag{9}$$

3. Radial Basis Function

A different method to compute the expansion coefficients is using Radial Basis Functions (RBF). RBF assumes a surrogate of the form:

$$c(\lambda) = \sum_{i=1}^{p} \alpha_i g_i(\|\lambda - \lambda_i\|) \tag{10}$$

where p is the number of sample points, α_i are coefficients to be determined. In principle, the kernel function $g_i(\|\lambda - \lambda_i\|$ can be any function of the norm between the required λ and the sampled λ_j. In this study, the multi-quadratic kernel was selected,

$$g_i(\|\lambda - \lambda_i\|) = \sqrt{\|\lambda - \lambda_i\|^2 + \gamma^2} \tag{11}$$

where γ is a shape parameter to be tuned. The coefficients α can be found by replacing the obtained values of c_i in Equation 10 and solving the resultant system of linear equations. Once α_i are obtained, which is done only once in the offline phase, values for c_i can be computed in the online phase for any new parameter λ. It is important to highlight that the selection of the shape parameter has an effect on the accuracy of the interpolation [14]. The shape parameter in this work was selected by dividing the data into a training set and a testing set. The parameter was then optimized by cross validation of the two sets to minimize the error.

III. RESULTS AND ANALYSIS

Two cases were chosen to test the proposed algorithm. In both cases, the two-group diffusion eigenvalue equation is solved. Assumptions of no up scattering and no fast fissions were made for the equation,

$$\begin{aligned} -\nabla \cdot D_1 \nabla \phi_1 + (\Sigma_{a1} + \Sigma_{12})\, \phi_1 &= \frac{1}{k}\, \nu\Sigma_{f2}\, \phi_2 \\ -\nabla \cdot D_2 \nabla \phi_2 + \Sigma_{a2}\phi_2 &= \Sigma_{12}\phi_1 \end{aligned} \tag{12}$$

where D_g is the group diffusion coefficient, Σ_{ag} is the group absorption cross section, Σ_{12} is the down scattering cross section, k is the multiplication factor, ϕ_1 and ϕ_2 are the fast and thermal flux respectively.

In each test case, Equation 12 is first solved with a well-established numerical method (Finite Difference in the first case and Finite Element in the second). Then, the reduced models (RBF and Smolyak) were built and assessed with respect to that reference solution. All computations were performed in a Matlab environment. It is important to note that in both cases the reference solution itself was fast enough to be solved inexpensively at any desired point. Thus, building a reduced order model was not required in those cases. Nevertheless, the test cases were selected for illustrative purposes only.

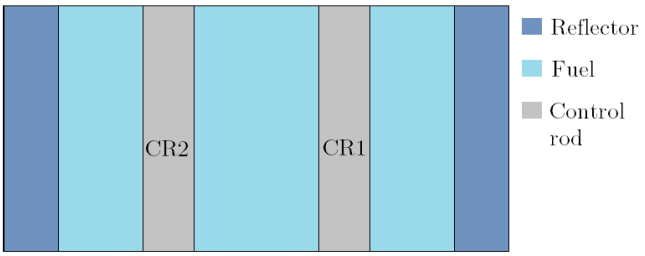

Fig. 2. Geometry of the slab in Case1.

1. Test Case 1

The first case is an eigenvalue problem solved with a Finite Difference scheme. Equation 12 is solved for one spatial direction. Figure 2 shows the slab geometry, which has a total thickness of 396 cm. The flux at the boundaries is assumed to be zero. The fuel region is reflected at both ends with a reflector of thickness 15.4 cm at each side. Two control rods are introduced in the fuel region, each with equal thickness of 15.4 cm. The domain was discretized into a total of 780 mesh points. The percentage insertion of each control rod is considered as an input parameter for the model. Thus, the model is parametrized on a 2D space. For this test case, only the thermal flux is considered as an output for the model. Nevertheless, the same algorithm can be applied to the fast flux.

The algorithm was applied to the model and resulted in a sparse grid level selection of 5 (145 points). The resulting singular values are shown in Figure 3. For comparison purposes, the singular values of the previous level ($l = 4$) are also plotted in the same figure. A close-up view of the first singular values can be seen in Figure 4. Indeed, by examining the singular values, it is evident that most of the points added in level 5 contributed only to the lower part of the plot. In fact, the algorithm revealed that the maximum absolute slope change between the two levels in the leading singular values was 0.03.

To build the reduced models, Equation 3 was first used to compute the expansion coefficients. Then, two nonintrusive models were built with the obtained POD modes and coefficients. The first was RBF with Equation 10 and the second was Smolyak's interpolant as in Equation 9. Both models were tested with 121 points that were not part of the training set. The maximum error in L_2 norm was found to be 17% for the RBF model and 9% for the Smolyak model. This case was observed when control rod 1 was inserted 30% and control rod 2 inserted 5%. Figure 5 shows the flux for this case. In Figure 6, a different selected point is shown where also the Smolyak model had outperformed RBF. The reference model had a runtime of around 10 s. On the other hand, both RBF and Smolyak models achieved a considerable saving in computational time. Smolyak model needed 0.1 s for a single

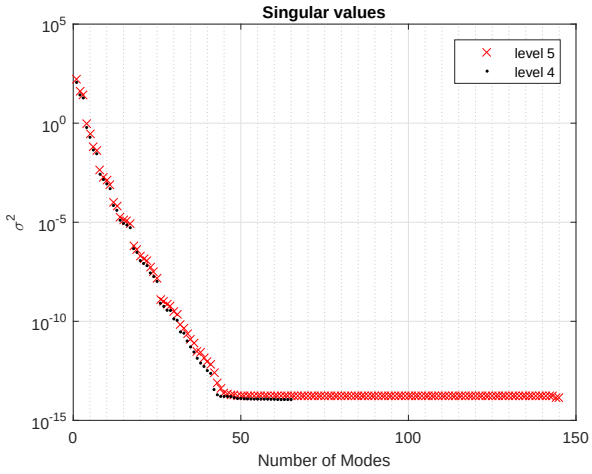

Fig. 3. Singular values of Case 1 for $l = 5$ (145points) compared with the previous level of $l = 4$ (65points).

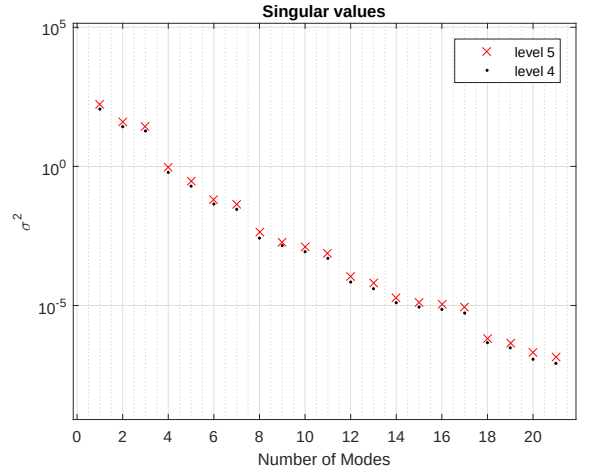

Fig. 4. A close-up view of the first singular values seen in Figure 3.

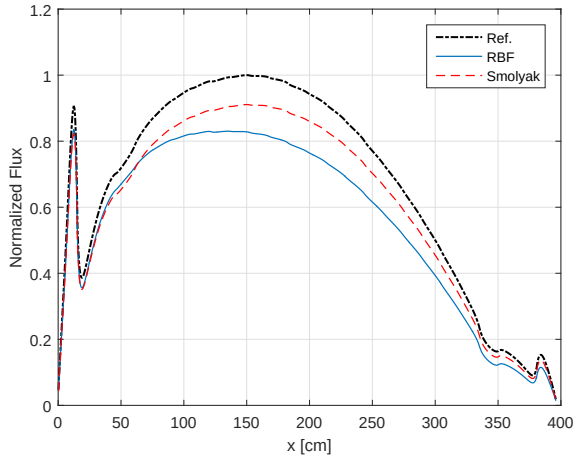

Fig. 5. Normalized thermal flux for Case 1. CR1 inserted 30% and CR2 inserted 5% (RBF error = 17% and Smolyak = 9%).

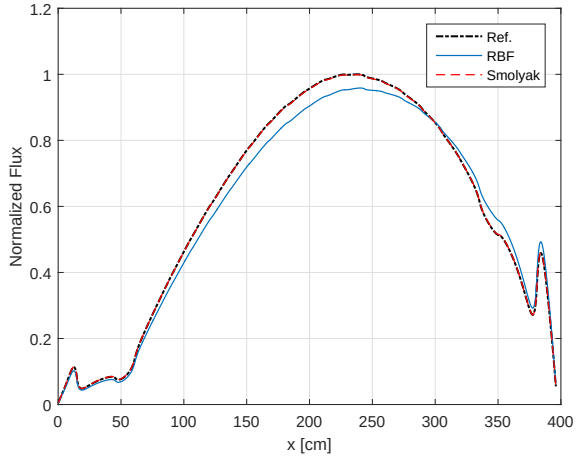

Fig. 6. Normalized thermal flux for Case 1. CR1 inserted 10% and CR2 inserted 60% (RBF error = 5% and Smolyak = 0.1%).

simulation. The RBF model was even faster than Smolyak by a factor of 10. The offline time to assemble both models was around 1451 s.

2. Test Case 2

The second tested case is the 2D IAEA benchmark problem as described in Ref. [15]. The core has two fuel zones with five control rods and a reflector. The geometry of the core can be seen in Figure 7. The steady state, 2-group diffusion equation (Equation 12) is solved in two spatial dimensions. The cross sections of the different regions are reported in Table II. The benchmark problem also provides the axial buckling $B^2_{z,g} = 0.8 \times 10^{-4}$. Thus, a term $D_g\, B^2_{z,g}$ is added to the removal term of Equation 12. The boundary conditions are assumed to be vacuum at the external boundary ($J^{\text{in}}_g = 0$) and symmetry at the inner boundaries ($\nabla\phi_g = 0$). This problem was solved with a Finite Element Method (FEM) on an unstructured mesh employed in a Matlab environment. The FEM model is considered as the reference model for the problem. The insertion percentage of the control rods were considered as input to the model. Thus, a nonintrusive reduced order model of the FEM is built with 5 input parameters corresponding to each control rod position. The model output was considered to be the thermal flux.

The algorithm selected sparse grid level 4, which resulted in 801 simulation points. The leading singular values are plotted in Figure 8 along with the singular values of the previous level. The figure shows the similarity of the decay between level 4 and level 3. This indicates that most of the new level points had little contribution to the dominant singular values. The resultant POD modes were truncated to $r = 50$ in order to build the reduced RBF and Smolyak models. The expansion coefficients were obtained by applying Equation 3. The models were then tested with 1500 points that were not part of the training set. The points were generated on a uniform full grid spanning the parameter domain. The error for both

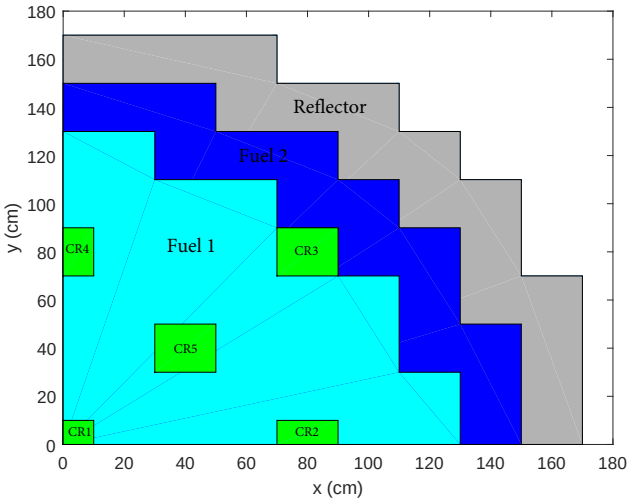

Fig. 7. Geometry of the 2D IAEA benchmark problem as implemented for Test Case 2.

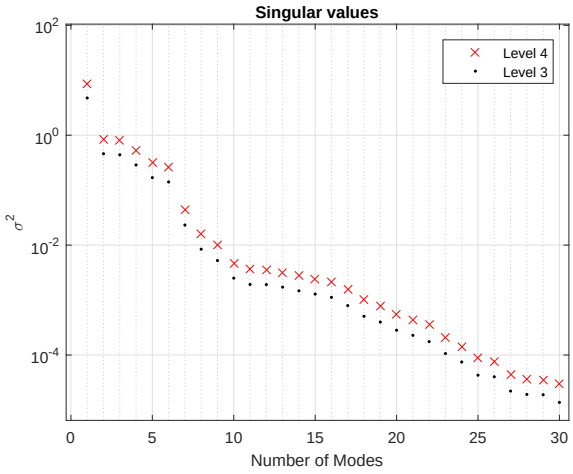

Fig. 8. Leading singular values for Test Case 2 plotted in comparison with the singular values of the previous level.

TABLE II. Cross Section data for the different regions in Test Case 2.

	Fuel 1	Fuel 2	Control Rod	Reflector
D_1 [cm]	1.5	1.5	1.5	2
D_2 [cm]	0.4	0.4	0.4	0.3
Σ_{12} [cm^{-1}]	0.02	0.02	0.02	0.04
Σ_{a1} [cm^{-1}]	0.01	0.01	0.01	0
Σ_{a2} [cm^{-1}]	0.08	0.085	0.13	0.01
$\nu\Sigma_{f2}$ [cm^{-1}]	0.135	0.135	0.135	0

models is compared in Figure 9. The reference FEM model computed a single simulation in about 3 s. RBF model needed 2404 s to assemble the model (offline time) and 0.005 s for a single simulation (online time). On the other hand, Smolyak model needed almost the same time for the offline phase and 0.3 s for the online phase. The results show that while RBF was faster in running a single simulation, Smolyak model outperformed RBF by a considerable margin. All error analyses were assessed in the L_2 norm. The average error for the RBF was 1.03% whereas the average Smolyak's error was found to be 0.08%. The maximum observed RBF error was 2.7%. The same configuration resulted in a Smolyak error of 0.04%. This case is shown in Figure 10. The flux is given along the x-axis and along the diagonal line ($y = x$). On the other hand, Figure 11 shows the configuration that resulted in a maximum Smolyak error, which was found to be 0.3%. This configuration resulted in an RBF error of 2.7%.

IV. CONCLUSIONS

Building a reduced order POD model for high dimensional problems can be achieved efficiently with the use of sparse grids. The suggested algorithm of comparing the singular values of the different spars grid levels provides a valuable tool for the efficient selection of the sampling points.

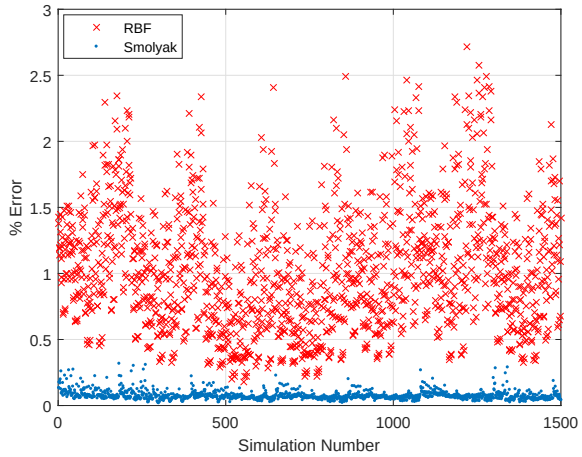

Fig. 9. Test Case 2 error comparison between RBF and Smolyak models for 1500 simulation points.

Thus, the offline time can be reduced significantly in problems parametrized on high dimensional spaces. Moreover, combining sparse grid sampling with Smolyak's combination technique results in an effective nonintrusive reduced order model. In this work, Smolyak's interpolant was tested with equally spaced nodes and piecewise linear interpolation. Also, a comparison with RBF was presented for two nuclear problems. In both cases, the results showed that while RBF resulted in a faster reduced order model, Smolyak's model provided a superior accuracy. Nevertheless, different RBF kernels were not studied and the shape parameter was selected by manual optimization. As suggested in Ref. [14], the accuracy of the RBF can be improved with advanced optimization.

Although the sparse grid approach generated an efficient set of sampling points compared to the full grid tensorization, the number of points still depends on the dimension d. As is evident from Table I, the number of points increases sharply with the increase in d and l. Therefore, the algorithm may

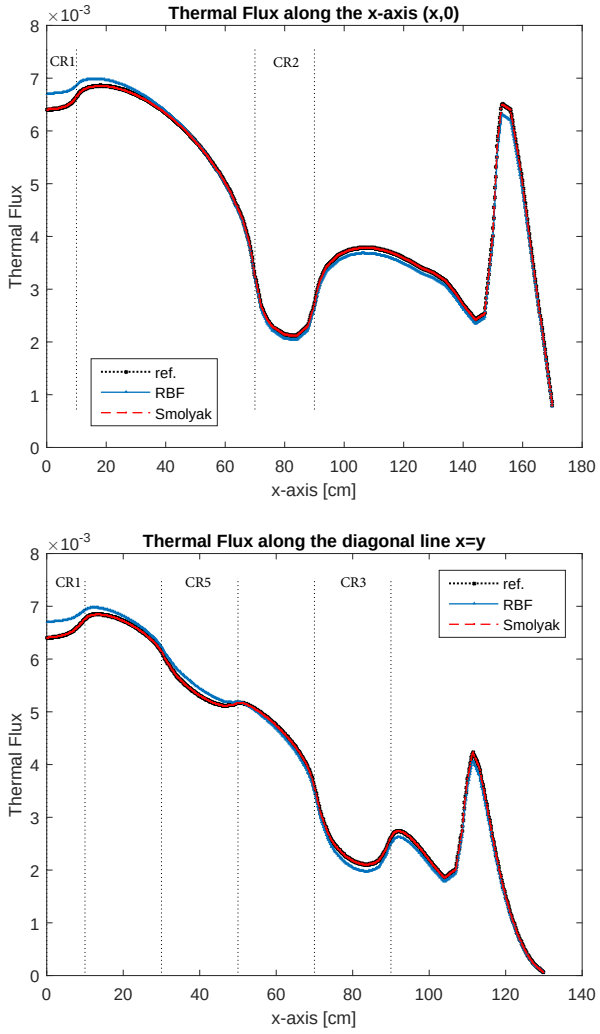

Fig. 10. Thermal flux for the configuration that resulted in a maximum RBF error in Test Case 2 (control rods insertion percentages were [$CR1$ = 10%, $CR2$ = 90%, $CR3$ = 58%, $CR4$ = 90%, $CR5$ = 10%]). RBF error was 2.7% and Smolyak's error was 0.04%.

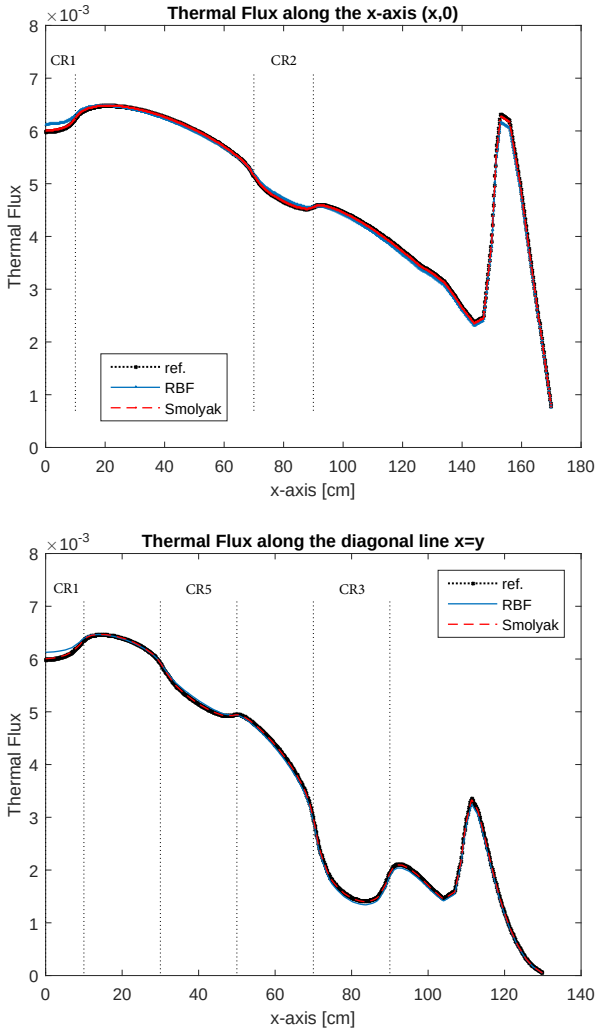

Fig. 11. Thermal flux for the configuration that resulted in a maximum Smolyak model error in Test Case 2 (control rods insertion percentages were [$CR1$ = 10%, $CR2$ = 10%, $CR3$ = 90%, $CR4$ = 10%, $CR5$ = 10%]). RBF error was 1.8% and Smolyak's error was 0.3%.

result in an infeasible number of simulations for really high dimensions. Similarly, models with strong nonlinearities will need a higher level of sparse grids. In these cases, adaptive sparse grids can be employed to increase the sampling points only in regions of higher interest. Therefore, in future work, we will investigate the use of adaptive sparse grids in building reduced order models.

REFERENCES

1. P. BENNER, S. GUGERCIN, and K. WILLCOX, "A Survey of Projection-Based Model Reduction Methods for Parametric Dynamical Systems," *SIAM review*, **57**, *4*, 483–531 (2015).
2. J. L. LUMLEY, "The Structure of Inhomogeneous Turbulent Flows," *Atmospheric Turbulence and Radio Wave Propagation*, **790**, 166–178 (1967).
3. A. BUCHAN, C. PAIN, F. FANG, and I. NAVON, "A POD Reduced-order Model for Eigenvalue Problems with Application to Reactor Physics," *International Journal for Numerical Methods in Engineering*, **95**, 1011–1032 (2013).
4. A. SARTORI, D. BAROLI, A. CAMMI, D. CHIESA, L. LUZZI, R. PONCIROLI, E. PREVITALI, M. E. RICOTTI, G. ROZZA, and M. SISTI, "Comparison of a Modal Method and a Proper Orthogonal Decomposition Approach for Multi-group Time-dependent Rreactor Spatial Kinetics," *Annals of Nuclear Energy*, **71**, 217–229 (2014).
5. H. V. LY and H. T. TRAN, "Modeling and Control of Physical Processes using Proper Orthogonal Decomposition," *Mathematical and Computer Modelling*, **33**, *1-3*, 223–236 (2001).
6. V. BULJAK, *Inverse Analyses with Model Reduction: Proper Orthogonal Decomposition in Structural Mechanics*, Springer, Berlin (2011).
7. M. GUÉNOT, I. LEPOT, C. SAINVITU, J. GOBLET, and R. FILOMENO COELHO, "Adaptive Sampling Strategies for Non-intrusive POD-based Surrogates," *Engineering Computations*, **30**, *4*, 521–547 (2013).
8. S. A. SMOLYAK, "Quadrature and Interpolation Formulas for Tensor Products of Certain Classes of Functions," in "Dokl. Akad. Nauk SSSR," (1963), vol. 4, pp. 240–243.
9. V. BARTHELMANN, E. NOVAK, and K. RITTER, "High Dimensional Polynomial Interpolation on Sparse Grids," *Advances in Computational Mathematics*, **12**, *4*, 273–288 (2000).
10. B. PEHERSTORFER, *Model Order reduction of Parametrized Systems with Sparse Grid Learning Techniques*, Ph.D. thesis, Technische Universität München, München (2013).
11. D. XIAO, F. FANG, A. BUCHAN, C. PAIN, I. NAVON, and A. MUGGERIDGE, "Non-intrusive Reduced Order Modelling of the Navier–Stokes Equations," *Computer Methods in Applied Mechanics and Engineering*, **293**, 522–541 (2015).
12. P. HOLMES, J. L. LUMLEY, and G. BERKOOZ, *Turbulence, Coherent Sructures, Dynamical Systems and Symmetry*, Cambridge University Press, Cambridge (1996).
13. A. KLIMKE, *Uncertainty Modeling using Fuzzy Arithmetic and Sparse Grids*, Ph.D. thesis, Universität Stuttgart, Stuttgart (2006).
14. P. CHANDRASHEKARAPPA and R. DUVIGNEAU, "Radial Basis Functions and Kriging Metamodels for Aerodynamic Optimization," Research report, INRIA (2007).
15. ARGONNE NATIONAL LABORATORY, "Argonne Code Center: Benchmark Problem Book," Anl-7416, Suppl. 2 (1977).